



Journal Homepage: -www.journalijar.com
**INTERNATIONAL JOURNAL OF
 ADVANCED RESEARCH (IJAR)**

Article DOI:10.21474/IJAR01/9127
 DOI URL: <http://dx.doi.org/10.21474/IJAR01/9127>



RESEARCH ARTICLE

GROUNDS OF A CONJUGATED META-NITROBENZALDEHYDE OF THIOSEMICARBAZONE, A RIBONUCLEOTIDE REDUCTASE AS A ROS GENERATOR AND APOPTOSIS INDUCER IN A549 NON-SMALL CELL LUNG CANCER CELL.

C. Jeevarathinam¹ and G. V. Pandian².

1. Department of Chemistry, Arignar Anna Govt. Arts & Science College, Karaikal.
2. Department of Chemistry, T.B.M.L College, Porayar.

Manuscript Info

Manuscript History

Received: 24 March 2019
 Final Accepted: 26 April 2019
 Published: May 2019

Key words:-

Solution Growth, Slow Evaporation Technique, Spectral Characterization, Microbial Activities, Anticancer Activity, Lung Cancer.

Abstract

Lung cancer is one of the primary causal agents of destruction among all diseases. More than 80% of lung cancer cases are non-small cell lung cancer (NSCLC) cases remaining 20% of lung malignant neoplastic disease are small cell lung cancer (SCLC). In search of potential therapeutics for cancer, we described herein the synthesis, characterization and *in vitro* anticancer activity of Meta-Nitrobenzaldehyde thiosemicarbazone (M-NBTSC). Meta-Nitrobenzaldehyde thiosemicarbazone is an interesting case of organic crystal. It has been grown by slow evaporation solution growth technique (SESGT) using wood alcohol as solvent. The MTT assay was applied to determine the IC₅₀ values on A549 lung cancer cell line by M-NBTSC. Features of apoptosis were observed by AO/EB and Hoechst staining. The caspase activity, Bcl-2 family, p21 and p53 proteins were measured by RT-PCR and Western Blot analysis. The M-NBTSC significantly inhibited the growth of A549 cells and induced apoptosis. The M-NBTSC was the most potent on A549 cell line with the IC₅₀ value of 50.50% cell viability 6µg/mL. The induction of apoptosis was overserved by chromosomal condensation, cell shrinkage, membrane blebbing and nuclear fragmentation. The answers showed that M-NBTSC induced apoptosis were associated with an upregulation of proapoptotic Bax and down regulation of Bcl2, dissipation of mitochondrial membrane potential and activation of caspase-3. In addition to diminished mitochondrial membrane potential and overproduction of ROS demonstrated the involvement of apoptosis. Mechanistic studies further revealed that M-NBTSC caused the growth of the intracellular ROS, consequently provoked the increase in p21 and p53 expression and led to upregulation of Bax, depolarization of mitochondrial membrane potential and caspases cascade (caspase-3/8 and -9). The increase of p53 level by M-NBTSC results in the inhibition of Ribonucleotide reductase (RR) enzymes and stimulates programmed cell death. In this survey suggest that M-NBTSC induces apoptosis through ROS-dependent and induce a potential healing effect for lung cancer.

Copy Right, IJAR, 2019,. All rights reserved.

Corresponding Author:-C. Jeevarathinam.

Address:-Department of Chemistry, Arignar Anna Govt. Arts & Science College, Karaikal.

Introduction.

Lung cancer is a major health problem of both genders accounting for about 14.1 million new cases diagnosed every year and approximately 8.2 million deaths being recorded worldwide in 2012. An estimated 221200 new instances of lung, malignant neoplastic disease are expected in 2015, accounting for about 13% of all cancer diagnoses. The 5-year survival for small cell lung cancer (6%) is lower than that for non-small cell lung cancer (21%). The two major kinds of lung, malignant neoplastic disease are small-cell lung cancer (SCLC) and non-small cell lung cancer (NSCLC), which comprise approximately 15 and 85% of all cases respectively. Despite the role of established and novel therapeutic strategies, such as surgery, chemotherapy and ionizing radiation therapy, the prognosis for NSCLC remains unsatisfactory. These data emphasize the demand for effective therapy for this disease. Numerous works have demonstrated that thiosemicarbazones are potent inhibitors of the enzyme ribonucleotide reductase and are capable of interrupting DNA synthesis and repair (12). The anticancer activities of thiosemicarbazone were closely linked to the parent aldehyde or ketone group, metal chelation ability and terminal amino substitution. Among them, the parent aldehyde or ketone group was considered decisive for the anticancer activity of thiosemicarbazone. Heterocyclic thiosemicarbazone showed higher activity compared with aromatic thiosemicarbazone [22]. An organic M-Nitrobenzaldehyde of thiosemicarbazone is an organic crystal play an important function in biological. In recent years, intense research study has been taken out to identify a limited sort of application oriented material. Organic compounds are frequently shaped by very weak Vander walls and hydrogen bonds and possess a high degree of delocalization. Hence, they are optically more nonlinear than inorganic crystals. Recent researches have brought up that organic crystals are bulky in size, strong, stable, and large nonlinear optical susceptibilities compared to the inorganic crystals in this probe, we applied the human A549 non-small cell lung cancer cell line as a model to study the molecular mechanisms of the effect of Meta-Nitrobenzaldehyde thiosemicarbazone (M-NBTSC) on the stimulation of apoptosis. The raw information resulting from these surveys suggests that ROS generation and MMP decrease are the earliest and necessary events for the initiation of M-NBTSC induced apoptotic signaling. These findings should support to explain the mechanisms underlying M-NBTSC induced apoptosis and provide a foundation for the therapeutic function of this compound for the chemotherapeutic agents.

Methods and Materials.**Synthesis of M-NBTSC:**

To a hot solution of thiosemicarbazide (1.82 g, 20 Mol) in 160 ml of methyl alcohol, added drop wise the solution of 3-Nitrobenzaldehyde (3.0224 g, 20 Mol) in 70ml methanol. The mix was stirred and refluxed for 4 hours, it was filtered and the filtrate was concentrated to half the volume under reduced pressure. Later on a slow evaporation of the concentrate at room temperature, crystals were collected by filtration, rinsed with cold ethanol and dried in vacuo. The filtrate was kept in the refrigerator and after several hours fine yellow colored powder was received. This merchandise was used further for various biological applications.

Characterization of Chemically Synthesized Compound.**UV – Visible Spectroscopy Analysis:**

The purity of chemically synthesized M-NBTSC compound was carried by measuring the UV-Visible spectra between 200-500 nm. UV-Visible spectroscopy analysis has been performed using a Perkin-Elmer Lambda-35 spectrophotometer operated at a settlement of 1nm as a function of response time.

FT-IR Analysis:

FT-IR is the most useful analysis for identifying types of chemicals that are either organic or inorganic. It can be given to the analysis of solids or liquids. The purified form of M-NBTSC was subjected to Fourier Transform Infra-Red Spectroscopy analysis of the analytic thinking of functional groups present in synthesized compound and the spectra was recorded in the 4000-400 cm⁻¹ scope. (St. Joseph's College, Tiruchirappalli).

Chemicals and Reagents:

Dulbecco's modified Eagle's medium (DMEM), fetal bovine serum (FBS), penicillin/streptomycin, DMSO (cell culture grade), MTT (dimethylthiazolyltetrazolium bromide), Acridine orange and Ethidium bromide was purchased from Hi Media Laboratories, Mumbai, India. Antibody to b-actin was from Santa Cruz (CA, USA).

Lung Cancer Cell Culture:

Non-small cell lung cancer (NSCLC) A549 cell line obtained from the National Centre for Cell Science, Pune, India. Cells were cultured in Dulbecco's modified Eagle's medium (DMEM) supplemented with 10% Fetal bovine serum (10% FBS) and 1% penicillin/ streptomycin in a 5% CO₂ humidified atmosphere at 37°C. Cell viability was determined by staining with 0.4% trypan blue solution and counting the cells using a hemocytometer.

Cytotoxicity Assay:

Cytotoxicity assay was done by using MTT [3-(4, 5-dimethyl- thiazol-2yl)-2, 5-diphenyl tetrazolium bromide] assay of Yuwan et al., 2004. For cytotoxicity assays, cells in monolayer containing approximately 1×10^4 were added to each well of a 96-well culture plate and incubated for overnight at 37°C with 5% CO₂. A549 cells were processed with a series of 1 to 10 µg/ml concentration of chemically synthesized Meta-Nitrobenzaldehyde Thiosemicarbazone (M-NBTSC) compound. After treatment for 24 h of incubation, 20 µL of MTT was added and then the cultures were further incubated for 4 hrs. MTT was aspirated and then 200 µL of DMSO was added to dissolve the formazan crystals. The absorbance was measured at 570 nm (Measurement) and 630 nm (Reference) using a micro plate reader (Bio-rad, USA). DMSO by itself was found to be non-toxic to the cellular phones. The results were gathered up in triplicate each and used to calculate the means and standard deviation.

Acridine Orange/Ethidium Bromide (AO/EB) Staining:

For measuring apoptosis level in the cells, 5×10^5 cells were seeded on cover slip in a 6-well plate and allowed to attach overnight. The adjacent day, the medium was substituted with fresh medium containing a deadly dose of M-NBTSC and incubated for 24 hrs. At the final stage of the incubation cover slip was removed from the culture plate and stained with 50 µL/ml of AO/EB was added and incubated at 37 °C with 5% CO₂ for 30 mins. The stained cover slip was washing with 1×PBS for removing excess dye. Cover slip was fixed on a glass slide and images of the cells were captured using 20× objectives under a fluorescence microscope (Carl Zeiss, Jena, Germany).

Hoechst Staining:

The A549 cells in logarithmic growth phase were seeded at a final concentration of 5×10^5 /mL in a 6-well culture plate. A549 cells were exposed to M-NBTSC (6 µg/mL) for 24 hrs. Then A549 cells were stained by Hoechst 33258, and the changes in the nuclei of cells were examined and photographed by using an inverted fluorescence microscope (Fluoid cell imaging station) (Wu et al., 2011).

Measurement of Reactive Oxygen Species (ROS) Level:

ROS generation in A549 cells was assessed by fluorescence and Spectrofluorometer microscope. For measuring total ROS level in the cells, 5×10^5 cells were seeded on a cover-slip in 6-well plate and taken into account to attach overnight. The following day, the medium was substituted with fresh medium containing a deadly dose of M-NBTSC and incubated for 24 hrs. At the final stage of the incubation cover - strip was removed from the culture plate and stained with 40 µM DCFH-DA for 30 min. The stained cover slip was washed with 1×PBS for removing excess dye. The cover - slip was fixed on a glass slide and images of the cells were captured using 20× objectives under a fluorescence microscope (Carl Zeiss, Jena, Germany). For measuring total ROS level in the cells, cells were seeded in a 6-well plate and taken into account to attach overnight. The following day, the medium was substituted with fresh medium containing a deadly dose of M-NBTSC and incubated for 24 hrs. Following incubations, the cells were harvested by trypsinization and washed with 1×PBS and resuspended in 1×PBS containing 10 µM DCFH-DA and incubated at 37°C for 45 minutes. Ultimately, it was read at excitation of 485 NM and emission at 520 NM using a spectrofluorometer (Horiba, Fluoromax 4 Spectrometer, and Germany) and a graph was plotted denoting the change in ROS level.

Assessment of Mitochondrial Membrane Potential ($\Delta\Psi_m$)

Mitochondrial membrane potential ($\Delta\Psi_m$) in A549 cells was assessed by spectrofluorometer and fluorescence microscope. For assessing the $\Delta\Psi_m$ potential, cells (5×10^5 /well) were sown on a cover-slip in 6-well plates and covered overnight for attachment. Following day, the old medium was put back with fresh medium containing a deadly dose of NBTSC and incubated for 24 hrs. At the final stage of incubation cover-slip was stained with 50 µl of Rhodamine-123 dye (10 mg/ml) for 30 min, excess dye was taken away by washing with 1×PBS and images of cells were captured using 20× objectives under a fluorescence microscope (Carl Zeiss, Jena, Germany). For assessing the $\Delta\Psi_m$, cells were seeded in 6-well plates and incubated overnight for attachment. Following day, the old medium was put back with fresh medium containing a deadly dose of m-NBTSC and incubated for 24 hrs. Cells were collected by trypsinization and resuspended in 1 ml of Rhodamine-123 solution (10 mg/ml Rhodamine-123 in 1×PBS) and

incubated for 30 minutes at room temperature. Ultimately it was read at excitation of 488 NM and emission at 525 NM using a spectrofluorometer (Horiba, Fluoromax 4 Spectrometer, and Germany).

Results.

UV Analysis Result:

The purity of chemically synthesized m-NBTSC compound was carried by measuring the UV-Visible spectra between 200-500 nm. The recorded UV-Visible spectrum proves the highly transparent nature of the material between 500-800nm. The UV-Visible spectrum of M-Nitrobenzaldehyde of thiosemicarbazone was recorded using Lambda 25 spectrometer and is shown in figure -1.

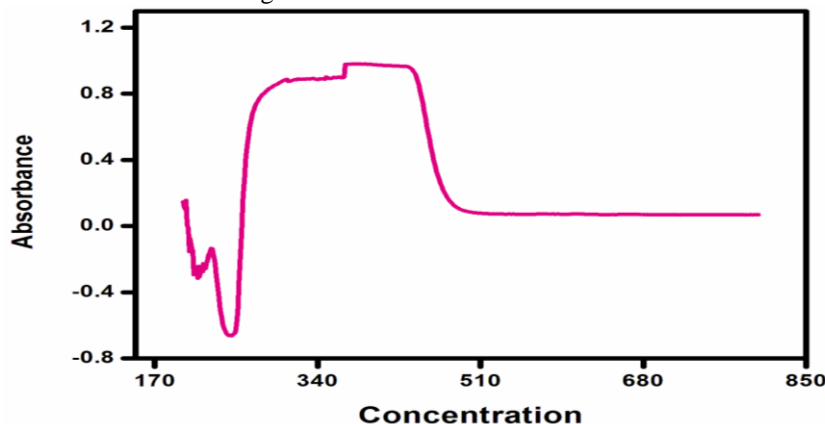


Figure 1: UV – Visible Spectrum of M-NBTSC

FT-IR Results:

Working groups present in the sample were analyzed using AVTAR370 DTGS FT-IR spectrometer in the wave number range from 400-4000 cm^{-1} using a KBr pellet technique. Fourier transform infrared (FT-IR) spectrum is an important book, which gives sufficient information about the construction of a compound. In this technique almost all working groups in a molecule absorb characteristic within a definite scope of frequency. The concentration of infrared radiation makes the various alliances in a molecule to stretch and bend with respect to one another. The Fourier Infra-red spectrum of the grown crystal is indicated in figure-2. The observed and their corresponding group identification is made in Table -1. The band obtained at 1600 cm^{-1} is due to the establishment of the amine group between M-Nitrobenzaldehyde and thiosemicarbazide. Referable to the C=N and N-N is stretching, vibration the peaks observed at below 1540 cm^{-1} . The peak observed in 1159.23 cm^{-1} shows C=S is stretching vibration. The peak observed at 1530 cm^{-1} . Shows the presence of -NO₂ group the peak corresponds to aromatic C-H was observed in 1298 cm^{-1} . At that point is, no peak observed at 2720 cm^{-1} confirms the aldehyde functional group in M-Nitrobenzaldehyde of thiosemicarbazone. The spectral data obtained for the thiosemicarbazone of benzaldehyde are well in accordance with theoretical and literature values.

Figure 2: FT-IR Spectrum of M-NBTSC.

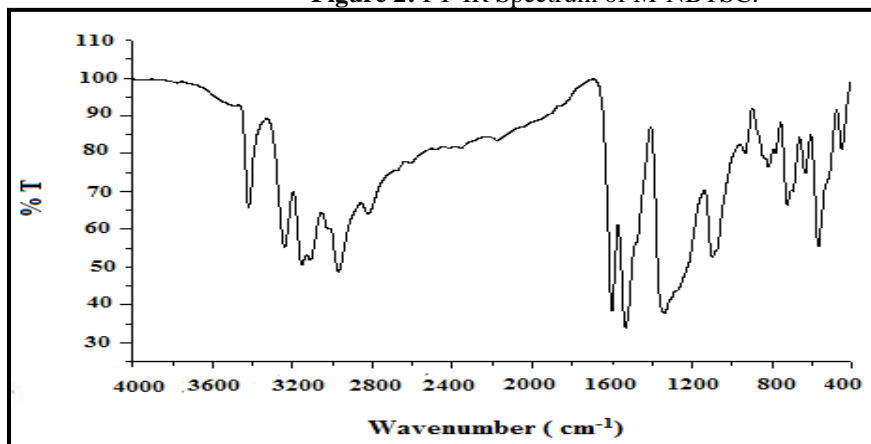
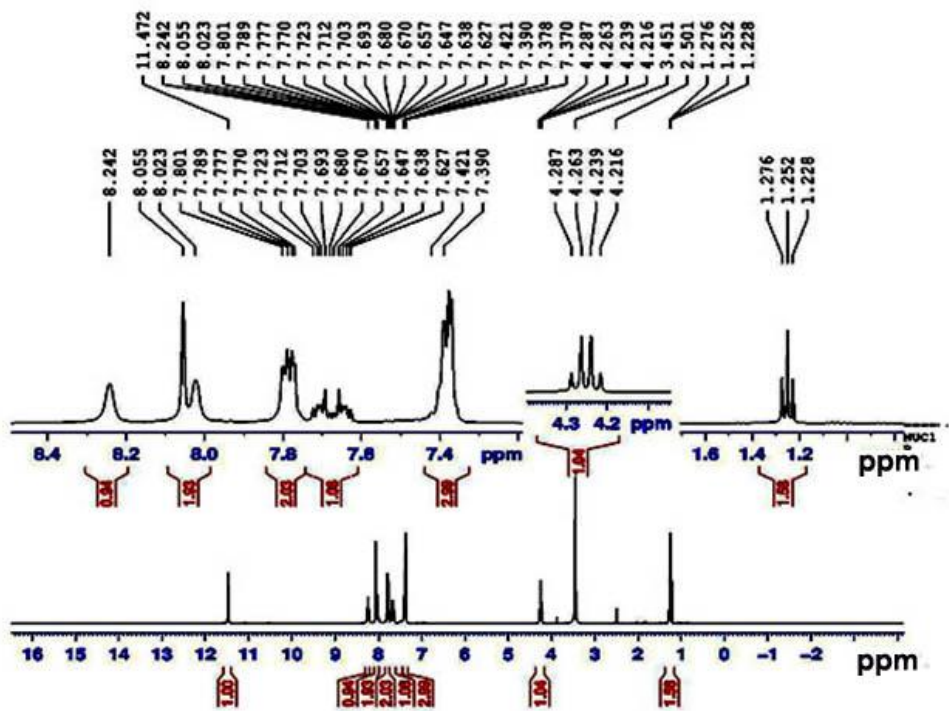


Table 1:-FT-IR Spectrum of M-NBTSC

S.No	Frequency cm^{-1}	Group Designation
1	3419	N-H amines group
2	3252	N-H Stretching
3	1298	Aromatic C-H
4	1540	N-N Stretching
5	1530	C-NO ₂ group
6	1600	C=N imine group
7	1159	C=S Stretching
8	1107	NH ₂ rocking

NMR Spectral Analysis.**¹H- NMR Spectral Analysis:**

The Nuclear Magnetic Resonance Spectral analysis is useful in the determination of the molecular structure based on the chemical environment of the magnetic nuclei such as ¹H, ¹³C, ³¹P etc., even at low concentrations. The ¹H NMR spectral analysis was run out of the M-Nitrobenzaldehyde of thiosemicarbazone in BRUKER 300 NMR spectrometer using DMSO as solvent. The ¹H NMR spectra of thiosemicarbazone of benzaldehyde is shown in figure 2.4 (a). A signal observed at $\delta=8.24\text{ppm}$ is corresponds to the NH₂ protons of hydroxide group. A singlet at $\delta=8.055\text{ ppm}$ confirm the NH proton. The multiplied observed between $\delta=7.370$ and 7.801ppm confirms the presence of aromatic protons. The presence of peak at $\delta=4.216\text{ ppm}$ indicates the HC=N protons. The signal at $\delta=3.451\text{ppm}$ shows the HOD signals of the solvent. The peaks at $\delta=1.276$ confirms the CH protons. The signal at $\delta=2.501$ indicates the residual protons present in DMSO d₆ solvent. The spectral data obtained from the M-Nitrobenzaldehyde of thiosemicarbazone is well in accordance with theoretical and literature values.

**Figure 3:-¹H-NMR Spectrum of M-Nitrobenzaldehyde of thiosemicarbazone****¹³C-NMR Spectral Analysis:**

The ¹³C NMR spectra of M-Nitrobenzaldehyde of thiosemicarbazone was recorded using BRUKER 300 NMR spectrometer using DMSO as solvent. The ¹³C NMR Spectrum of M-Nitrobenzaldehyde of thiosemicarbazone is

shown in figure 2.4 (b). The imine group is represented by the signal at $\delta=167.01$ ppm. The multiple peak at $\delta=127.36-134.74$ ppm represents the bearing of the benzene ring. The bearing of a peak at $\delta=13.94$ ppm confirms the substituted aromatic compound. The presence of residual protons present in DMSO d6 observed at $\delta=40$ ppm. The absence of peak at 25 and 17ppm confirms the absence of the methylene aliphatic group. The correlation of the signals observed in ^1H and ^{13}C NMR spectra with the functional group is presented in Table 2.4 (b). This correlation is well in accordance with the theoretical and standard values.

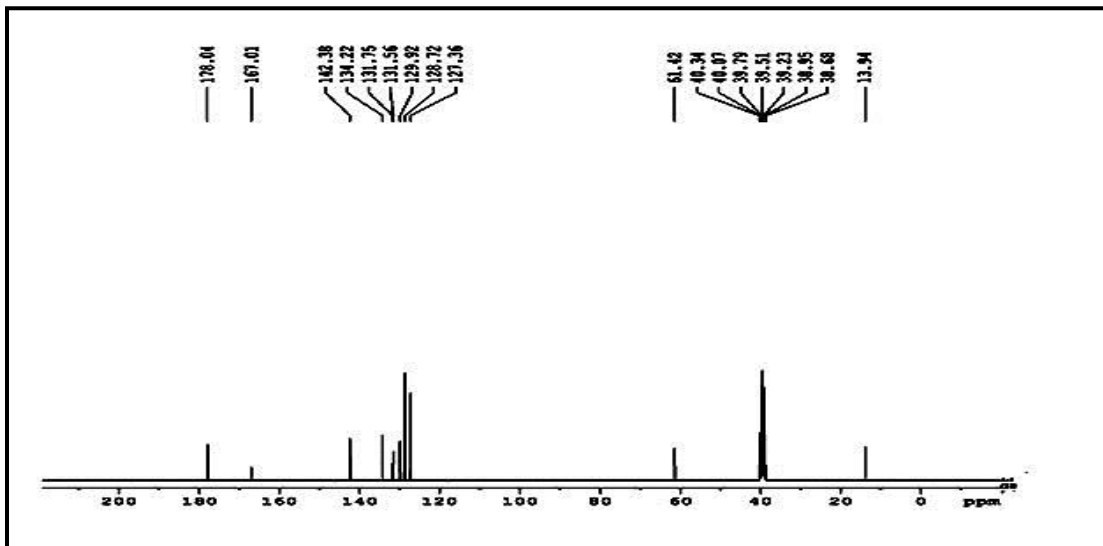


Figure 4:- ^{13}C -NMR Spectrum of M-Nitrobenzaldehyde of thiosemicarbazone

Table 2:-NMR Spectral Data of M-Nitrobenzaldehyde of thiosemicarbazone

Spectrum	Signal at δ ppm	Group identification
^1H	8.242	NH_2 proton of hydrazide
	8.055	NH-proton
	7.370-7.801	Aromatic protons
	4.216	HC=N protons
	1.276	CH protons
^{13}C	167.01	Imine group
	142.38	C=S group
	127.36-134.74	Benzene ring
	13.94	Substituted aromatic compound

Inhibitory Effects of M- NBTSC on A549 Cell Growth.

In vitro growth effects of M-NBTSC on lung cancer cells were evaluated using the MTT assay. The MTT assay as a screening method has been widely applied to assess the viability and proliferation of cells. M-NBTSC concentrations ranging from 1 to 10 $\mu\text{g}/\text{mL}$. The cell viability was decreased by M- NBTSC in a concentration-dependent manner for 24 hours. The IC_{50} concentration was found to be 6 $\mu\text{g}/\text{mL}$. Then, for further studies we selected 6 $\mu\text{g}/\text{mL}$ to identify the mechanism action of M-NBTSC in A549.

Cytomorphological Changes in A549 Cells.

The diverse morphological alteration was observed in M-NBTSC treated A549 cells, However, no such effects were seen in control cells. It was established that the morphological variations were discovered such as loss of membrane integrity, inhibition of cell growth, cytoplasmic condensation and cell clumping (Figure 8 B) results indicate that the M-NBTSC treated A549 cells undergone cell death, whereas the non-treated cells were active (Figure 8 A).

AO/EB Staining.

A549 cells were stained by AO/EB after 24 h treatment of M-NBTSC. The live, apoptotic and necrotic cells were monitored under the fluorescent microscope. Live cells appear uniformly green, whereas early-stage apoptotic cells,

marked by granular yellow, green AO nuclear staining, were detected in the experimental group (Figure 1B). Staining was localized irregularly within the cubicles. Late-stage apoptotic cells, with localized orange nuclear EB staining, were also detected in M-NBTSC treated group. These psychological changes indicated that the cells were charged to a specific mode of cell destruction, probably apoptosis leads to M - NBTSC were compared to untreated cells shows figure.

Hoechst Staining.

As shown in Figure 3, M-NBTSC treatment has induced apoptosis in a lethal dosage for 24 hours, exhibited bright blue color because of chromatin condensation, nuclear fragmentations and apoptotic bodies were clearly seen upon Hoechst 33258 staining. Control cells were seen with uniformly light blue nuclei under fluorescence microscope. These cytological changes indicated that the cells were committed to an exact mode of cell death, probably apoptosis.

Determination of Intracellular Reactive Oxygen Species (ROS) Level.

The generation of ROS plays a lively role in the cancer. Thus, the effect of ROS generation induced by M-NBTSC was investigated. ROS generation in A549 cells was significantly increased after M- NBTSC treatment compared with the levels of the control (Fig. 2). The increased ROS production was significantly decreased in control. ROS have vital functions in cellular signaling and homeostasis. At low concentration ROS promotes cancer cell survival by activation of growth factors and MAP-kinases (MAPKs) that further activates cell cycle progression. At high concentration ROS produces oxidative stress that triggers programmed cell death or apoptosis.

Reduction of Mitochondrial Membrane Potential (MMP) by M-NBTSC.

Cells stained with the Rhodamine-123 dye were analyzed by fluorescence microscope and spectrofluorometer. A decrease in the MMP is indicated by a diminution in the green fluorescence intensity ratio. Fig. 5 shows that M-NBTSC significantly depolarized the mitochondrial membrane of the cancer cells after 24 h incubation.

M-NBTSC Treatment Resulted in a Transition in the Levels of Bcl-2 Family Proteins in an A549 Cell.

As recorded by western blot analysis and its densitometry quantitation (Fig. 4), M-NBTSC treatment of A549 cell lines resulted in a decrease in antiapoptotic Bcl-2 and an associated with an increase in proapoptotic Bax proteins, thereby making a substantial growth in the Bax/Bcl-2 ratio that favors apoptosis. Our data clearly show that NBTSC causes an increment in the protein levels of proapoptotic members of the Bcl-2 family. These results confirmed the induction of apoptosis, resulted from the NBTSC treatment A549 cells.

Determination of Caspases Action on M-NBTSC.

The A459 cells were incubated with NBTSC the lethal dosage for 24 h, Caspase-9 expression was increased by M-NBTSC (Fig. 4A). Accordingly, caspase-3 activities were enhanced by M-NBTSC. Caspase-9 overexpression and its activation lead to apoptosis. These results further confirmed that M-NBTSC induced apoptosis. Since the majority of cancer therapy treatments initiate apoptosis through the caspase-9 activation. But, caspase-8 there was no change in NBTSC treatment for 24 hours in that results we confirmed the apoptosis thought the intrinsic pathway.

Effect of M-NBTSC on p21 and p53.

Apoptosis induced by p21 can be realized in p53-dependent or independent manner and by a direct activation of pro-apoptotic proteins. M-NBTSC induced expression of p21 was seen through the analytic thinking of reverse transcriptase-PCR. As recorded in Figure 19 A, the result clearly shows that p21 activity was increased. The resolution suggests that activation of p21 is highly induced in M-NBTSC mediated apoptosis.

Treatment.

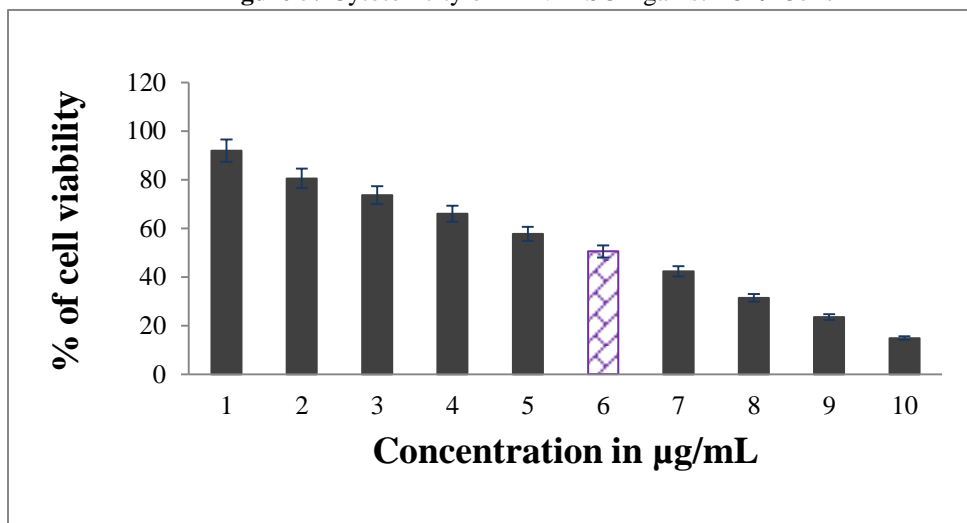
Ribonucleotide reductase (RR) is an enzyme, responsible for the formation of deoxyribonucleotide from ribonucleotide via reduction, starting material for DNA synthesis [6]. Ribonucleotide reductase inhibition offers an important therapeutic drug target for anticancer drugs. Thiosemicarbazone were attributed to the inhibition of ribonucleotide reductase, an enzyme involved in the rate-determining step of DNA synthesis. Thiosemicarbazones have shown significant antitumor activity against a profound bit of human tumor cell lines under in vitro conditions [16]. In the present study, we looked into the effects of M-NBTSC on NSCLC A549 cells and demonstrated that M-NBTSC inhibits A549 cell growth, an issue related to apoptosis induction. Programmed cell death is characterized by morphological changes such as membrane blebbing, cell shrinkage, chromatin condensation and DNA

degradation followed by rapid engulfment of cell debris by neighboring cells [17]. Induction of apoptosis in cancer cells is one of the useful strategies for anticancer drug development [18]. Therefore, we examined whether M-NBTSC induced cytotoxicity on A549 cells through the induction of programmed cell destruction. In our study, chromatin condensation of the nuclei, DNA fragmentation, cell shrinkage was observed in the M-NBTSC treated A549 cell lines. The IC₅₀ value of M-NBTSC, determined by stimulating A549 cells for 24 h, was 6 μ g/ml. IC₅₀ dose were used to look out over the morphological alteration. Apoptotic features such as chromosomal condensation, an inter nucleosomal syringe and DNA fragmentation were observed. The intrinsic apoptosis pathway is dependent on the release of apoptotic genes such as cytochrome c from the mitochondria to the cytosol, which is believed to be an initiator of the caspase cascade. Releasing apoptotic factors into the cytosol requires members of the Bcl-2 family, which is composed of pro- and anti-apoptotic proteins [6,27]. To confirm whether the intrinsic pathway is involved in M- NBTSC induced apoptosis, the effect of M-NBTSC on the reports of anti-apoptotic Bcl-2, pro-apoptotic protein Bax and cytochrome c was monitored. As suggested in Figure 5A, the total levels of Bax and Bcl-2 proteins remained unchanged in response to M-NBTSC treatment. However, M-NBTSC treatment decreased cytosolic levels of Bax, while its mitochondrial levels significantly increased after treatment with M-NBTSC (Figure 5B). Cytochrome c was also tested in mitochondrial and cytosolic fractions, as described in Figure 5B. M-NBTSC treatment caused a pronounced decrease in mitochondrial cytochrome c and a concurrent increase in cytosolic cytochrome c (Figure 5B). M-NBTSC was prepared by using M-Nitrobenzaldehyde and Thiosemicarbazide in methanol solution by taking a standard procedure. The crystal was grown by slow evaporation solution growth technique (SESGT). The presence of M-Nitrobenzaldehyde group and the nature of the protons were identified by FT-IR and ¹³C; ¹H NMR Spectral analysis. The UV-Visible spectrum reveals that the compound is chemically pure and coherent in the wavelength area.

Table 3:-Cytotoxicity of M-NBTSC Against A549 Cells:

Concentration of Compound (μ g/mL)	Cell Viability (%)
1	91.93
2	80.53
3	73.66
4	65.99
5	57.78
6	50.50
7	42.38
8	31.40
9	23.51
10	14.89

Figure 5:-Cytotoxicity of M-NBTSC Against A549 Cells



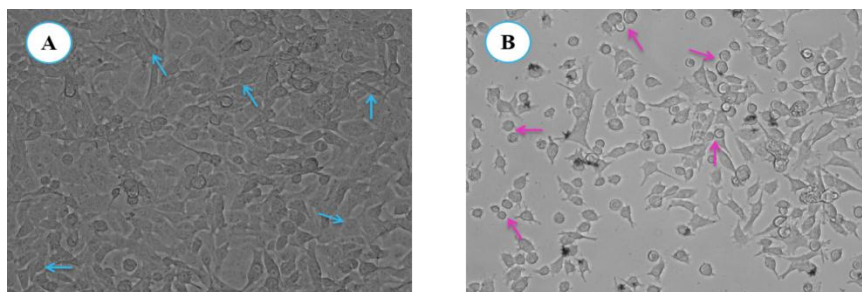


Figure 6:-Microscopic Images of M-NBTSC Induced Gross Cytomorphological Changes and Growth Inhibition at 24 h on the A549 Cells [Magnification at 20x; (A) Control; (B) M-NBTSC Treated]

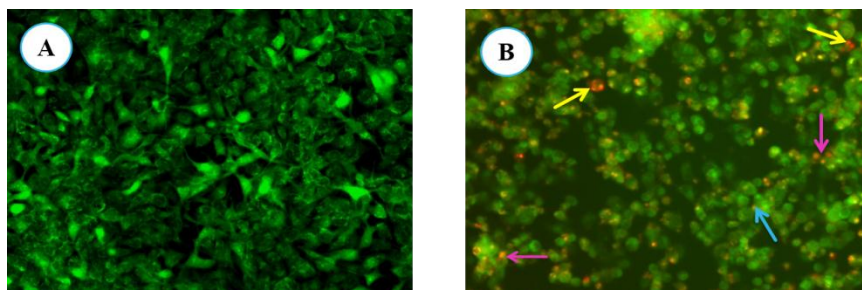


Figure 7:-AO/Et Br Staining of A549 Cells [Magnification at 20x; (A) Control; (B) M-NBTSC Treated]

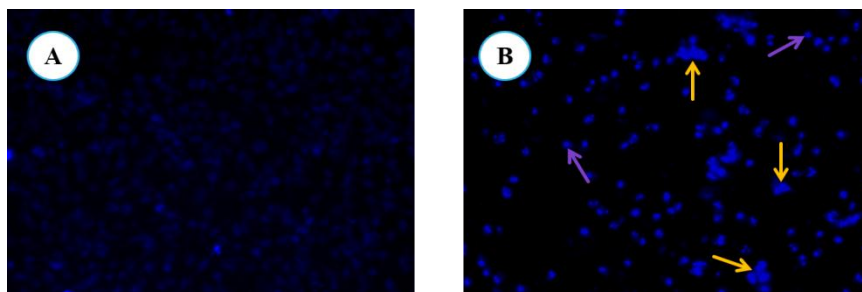


Figure 8:-Hoechst Staining of A549 Cells [Magnification at 20x; (A) Control; (B) M-NBTSC Treated]

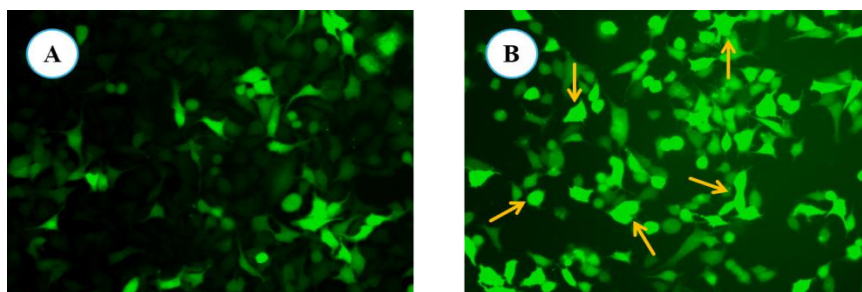


Figure 9:-ROS Generation in A549 Cells by M-NBTSC Using Fluorescent Microscope [Magnification at 20x; (A) Control; (B) M-NBTSC Treated]

Figure 10:-Measurement of ROS Level by Spectrofluorometric Method

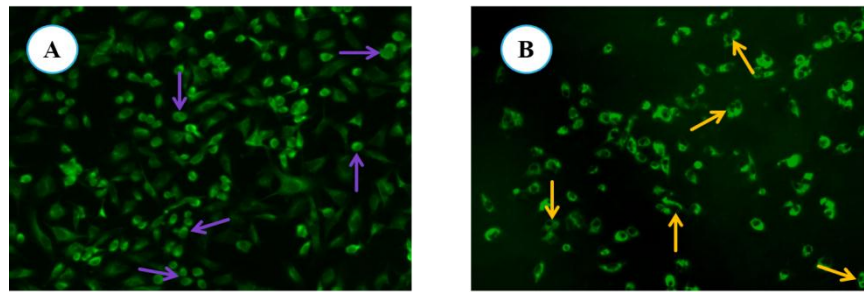
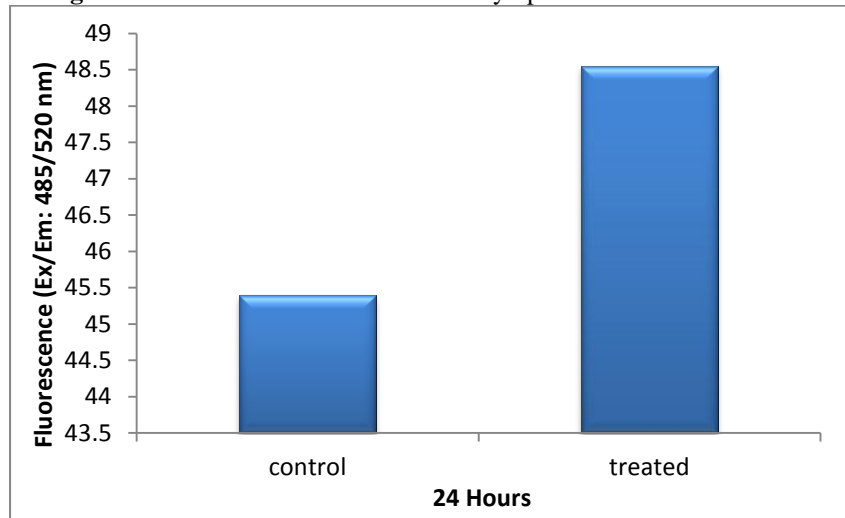
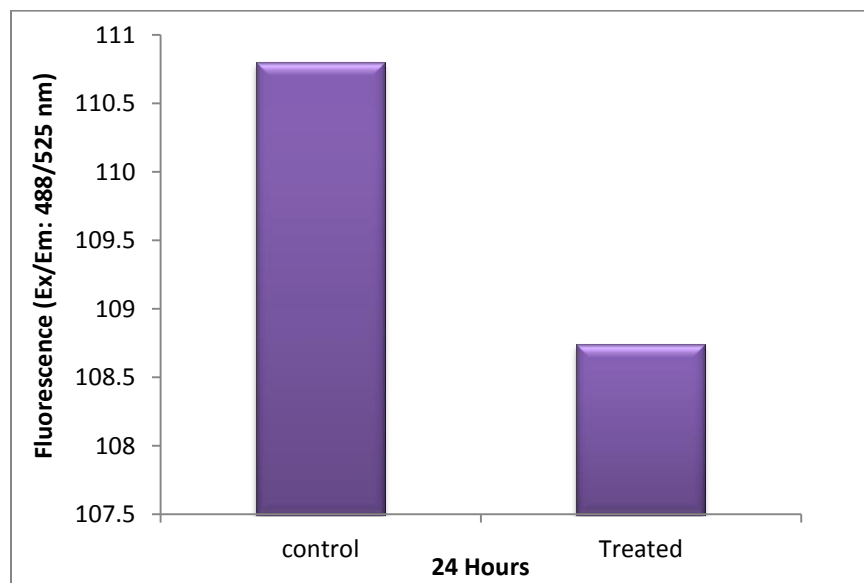


Figure 11:-Assessment of MMP level ($\Delta\psi_m$) in A549 Cells by M-NBTSC Treatment Using Fluorescent Microscope [Magnification at 20x; (A) Control; (B) M-NBTSC Treated]

Figure 12:-Measurement of MMP Level by Spectrofluorometric Method Pro-Apoptotic Factors



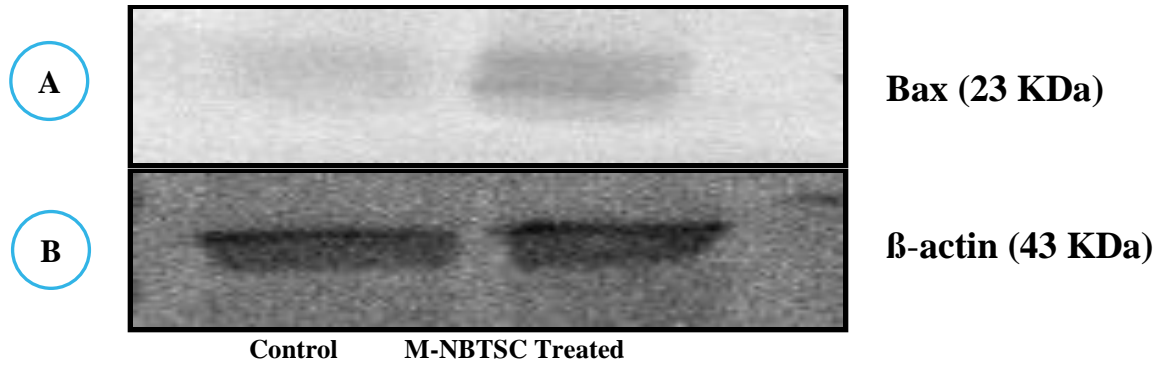


Figure 13:-Effect of M-NBTSC on Bcl-2 Family Proteins. Western Blot Was Performed for (A) Bax (B) β -actin (β -actin was used as Internal Command)

Figure 14:-Measurement of Bax (Bcl-2 Family Protein) Expression Level Intrinsic Pathway (Main Initiator)

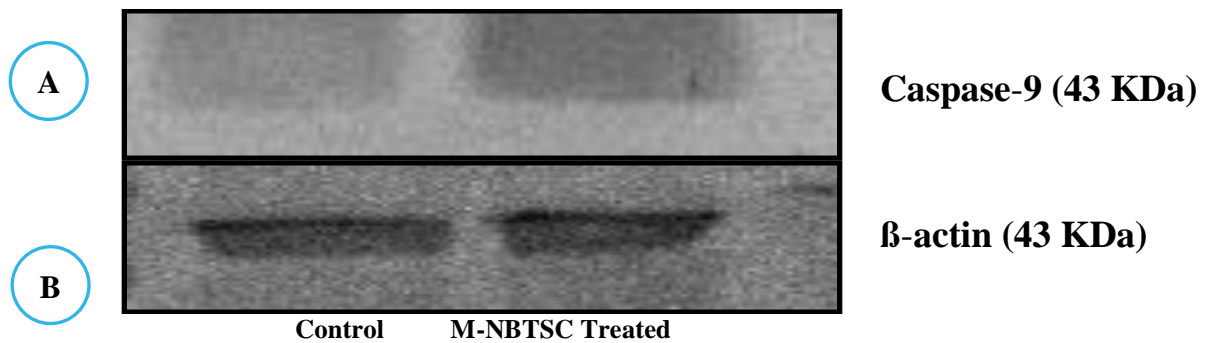
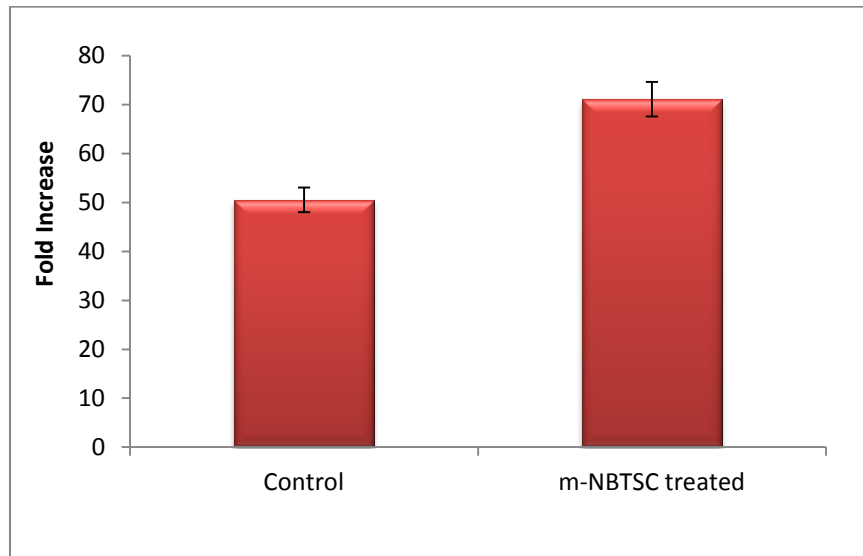


Figure 15:-Effect of M-NBTSC on Caspase-9. Western Blot was Performed for (A) Caspase-9 and (B) β -actin (β -actin was used as Internal Control)

Figure 16:-Measurement of Caspase-9 (Protein) Expression Level

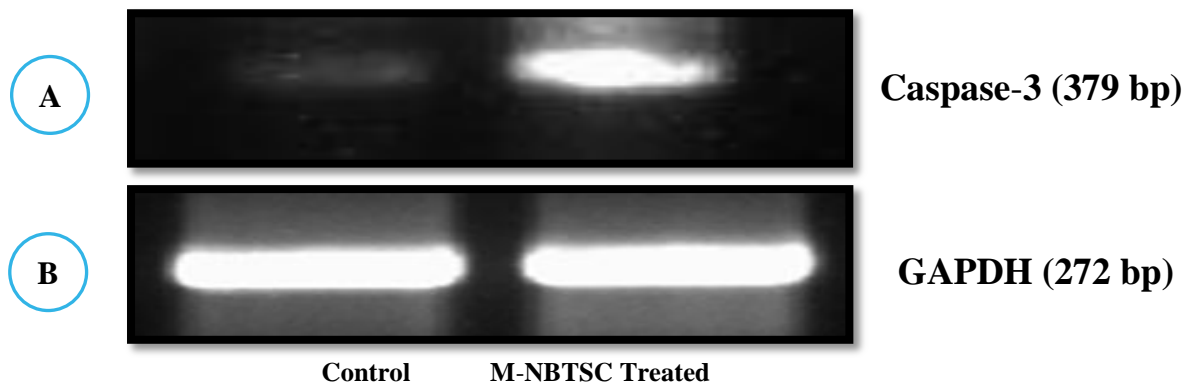
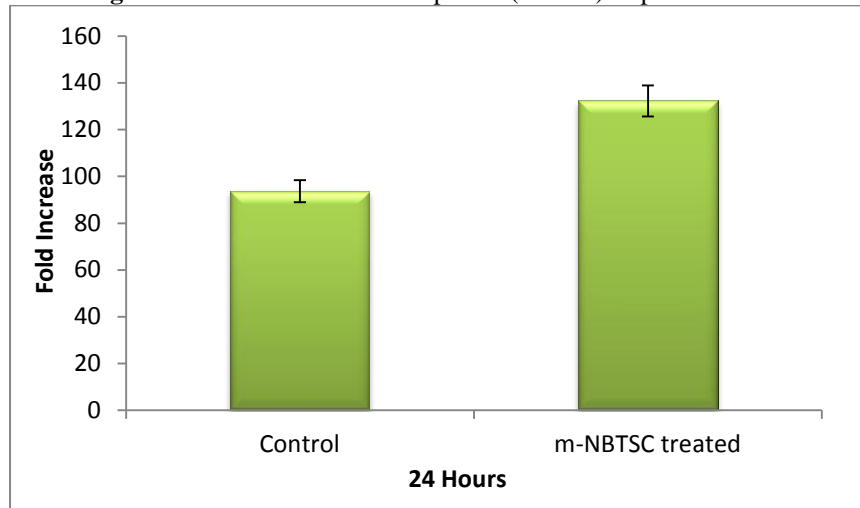
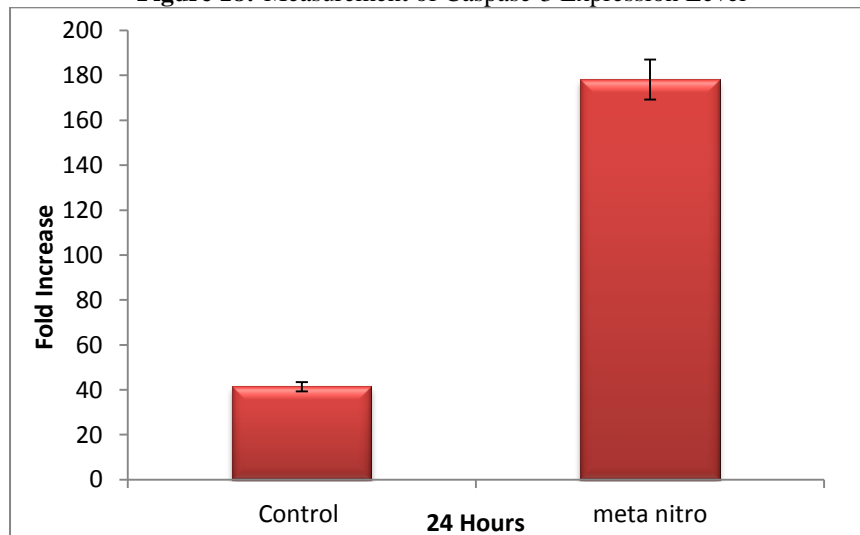


Figure 17:-Effect of M-NBTSC on Caspase-3. Reverse Transcriptase PCR Analysis was Performed for (A) Caspase-3 and (B) GAPDH (GAPDH was used as Internal Command)

Figure 18:-Measurement of Caspase-3 Expression Level



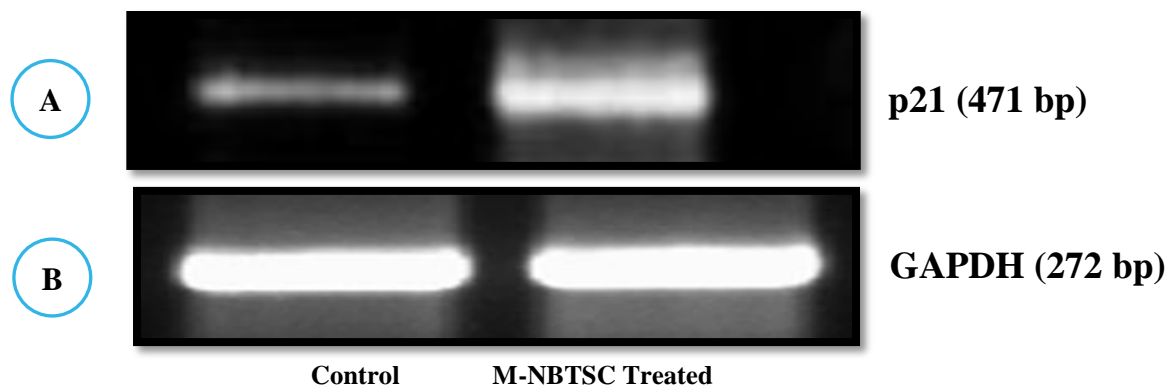
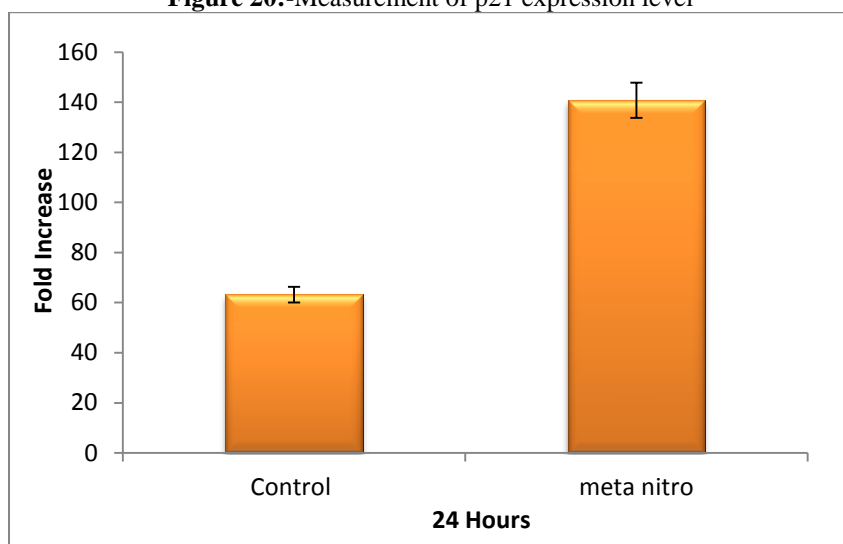


Figure 19:-Effect of M-NBTSC on p21. Reverse Transcriptase PCR analysis performed for (A) p21 and (B) GAPDH (GAPDH was used as Internal Control)

Figure 20:-Measurement of p21 expression level



Conclusion:-

In closing, with involves the exciting of the intrinsic pathway through the production of ROS, loss of mitochondrial membrane potential, cytochrome C release, inhibition of antiapoptotic proteins and overexpression of p53 and p21, Bax with the activation of caspase- 3. To our knowledge, these results clearly, investigation of M-NBTSC intensifies propose that induction of apoptosis in A549 could be linked showed for the first time that M-NBTSC induce apoptosis in lung cancer cells. The new data resulting from these studies indicates that ROS generation and loss of MMP are the earliest and necessary events for the initiation of M-NBTSC induced apoptotic signaling. These findings should support to explain the mechanisms underlying M-NBTSC induced apoptosis and provide a base for the remedial use of this compound for the chemotherapeutic agent.

Recognition:-

One of the authors (GVP) thank the University Grant Commission, New Delhi for the award of UGC: minor project [File No. 4- 1/2008 (BSR)]. The authors thank the management and principal of T. B. M. L. College for their support. The authors are grateful to the Dr. Brindha Department of Center for Advanced Research in Indian System of Medicine (CARISM).

References:-

1. Anbusrinivasan P, Pandian G.V, Determination of Nucleation Temperature, metastablezonewidth spectral analysis of sulphanic acid grown from Ethanol-Water as growth medium; Ultra chemistry, Vol 8 (1), 83-90 (2012).

2. RamachandraRaja C, Ramamoorthi K, R. Manimekalai, Growth and spectroscopic characterization of ethylene diamine tetra acetic acid (EDTA) doped Zinc sulphatehepta hydrate-A semi organic NLO material, *Spectrochimica Acta Part A* 99 (2012)23-26.
3. Madhurambal G ,Ramasamy P, Anbusrinivasan P,Vasudevan G, Kavitha S,Majumdar SC,Growth and characterization studies of Bromo-4^{'''}-Chloro acetophenone crystals. *J Therm Anal calorim* 2008; 94:59-62.
4. Vasudevan G , Anbusrinivasan P , Madhurambal G ,Mojumdar SC .Thermal analysis effect of dopants Spectral characterization and development aspect of KAP crystals.*J Therm Anal Calorim* 2009 (96) 99-102.
5. Ramalingam S, Anbusrinivasan P, Periandy S: FT-IR and FT-Raman Spectral Investigation, Computed IR-Intensity and Raman activity analysis and frequency estimation analysis on 4-chloro-2-bromoacetophenone was – HF and DFT calculations; *Spectrochimica Acta part A* 2011 (78) 826-834.
6. Manivannan S, Danuskodi S. Growth and characterization of a new organic nonlinear crystals: Semicarbazone of N-dimethylaminebenzaldehyde *J.Crystal growth* 257 (2003) 305-308.
7. Jaikumar.D, Kalainathan.Bhagavanarayana.G“Synthesis, growth, thermal, optical and mechanical properties of new organic NLO crystal: L-alanine DL-malic acid ,”*J. Cryst. Growth*, 312(2009) 120–124
8. Pundir, R.K., Jain, Pr. and Sharma, Ch. (2010) Antimicrobial Activity of Ethanolic Extracts of *Syzygium aromaticum* and *Allium sativum* against Food Associated Bacteria and Fungi. *Ethnobotanical Leaflets*, 14, 344-360.
9. V. Krishnakumar, R. John Xavier, *Spectrochim. Acta A* 61 (2005) 253-260.S.Wanninger, V.Lorenz, A.Subhan and F.T.Edelmann , Metal complexes of curcumin – synthetic strategies, structures and medicinal applications, 2015
10. Obregón-Mendoza, M.A., Estévez-Carmona, M.M., Hernández-Ortega, S., Soriano-García, M., Ramírez-Apán, M.T., Orea, L., Pilotzi, H., Gnecco, D., Cassani, J. and Enríquez, R. (2017) Retro-Curcuminoids as Mimics of Dehydrozingerone and Curcumin: Synthesis, NMR, X-Ray, and Cytotoxic Activity. *Molecules*, 22, 33-47. .
11. R.Waranyoupalin, S.Wongnawa, M. Wongnawa, C. Pakawatchai,P. Panichayupakaranant and P. Sherdshoopongse, *CENT.EUR. J. CHEM.*, 2009, 7, 388–394.
12. Kikuzaki, H., Hisamoto, M., Hirose, K., Akiyama, K. and Taniguchi, H. (2002) Antioxidant Properties of Ferulic Acid and Its Related Compounds. *Journal of Agricultural & Food Chemistry*, 50, 2161-2168.
13. Jirovetz, L., Buchbauer, G., Stoilova, I., Stoyanova, A. and Schmidt, E. (2006) Chemical Composition and Antioxidant Properties of Clove Leaf Essential Oil. *Journal of Agricultural and Food Chemistry*, 54, 6303-6307.
14. Mancuso, C. and Santangelo, R. (2014) Ferulic Acid: Pharmacological and Toxicological Aspects. *Food and Chemical Toxicology*, 65, 185-195. <https://doi.org/10.1016/j.fct.2013.12.024>
15. Lai, H.Y., Yau, Y.Y. and Kim, K.H. (2010) *Blechnum orientale* Linn-A Fern with Potential as Antioxidant, Anticancer and Antibacterial Agent. *BMC Complementary and Alternative Medicine*, 10, 1-8.
16. M. K. Mishra, P. Sanphui, U. Ramamurty and G. R. Desiraju, *CRYST. GROWTH DES.*, 2014, 14, 3054–3061, and references cited therein.
17. E. Ferrari, B. Arezzini, M. Ferrali, S. Lazzari, F. Pignedoli, F. Spagnolo and M. Saladini, *BIOMETALS*, 2009, 22, 701–710.
18. J. Annarjai, S. Srinivasan, K. M. Ponvel and P. R. Athappan, *J. INORG. BIOCHEM.*, 2005, 99, 669–676, and references cited therein.
19. J. Rajesh, A. Gubendran, G. Rajagopal and P. Athappan, *J. MOL. STRUCT.*, 2012, 1010, 169–178.
20. Humini, K.N., Hamdane, R., Boutoutaou, R., Kihal, M. and Henni, J.E. (2014) Antifungal Activity of Clove (*Syzygium aromaticum* L.) Essential Oil against Phytopathogenic Fungi of Tomato (*Solanum lycopersicum* L.) in Algeria. *Journal of Experimental Biology and Agriculture Sciences*, 2, 447-454.
21. 18) E. Ferrari, R. Benassi, S. Sacchi, F. Pignedoli, M. Asti and M. Saladini, *J. INORG. BIOCHEM.*, 2014, 139, 38–48.
22. M. Asti, E. Ferrari, S. Croci, G. Atti, S. Rubagotti, M. Iori, P. C. Capponi, A. Zerbini, M. Saladini and A. Versari, *INORG. CHEM.*, 2014, 53, 4922–4933.
23. K. Mohammadi, K. H. Thompson, B. O. Patrick, T. Storr, C. Martins, E. Polishchuk, V. G. Yuen, J. H. McNeill and C. Orvig, *J. INORG. BIOCHEM.*, 2005, 99, 2217–2225.
24. Y. Sumanont, Y. Murakami, M. Tohda, O. Vajragupta, H. Watanabe and K. Matsumoto, *BIOL. PHARM. BULL.*, 2007, 30, 1732–1739, and references cited therein.
25. R. Pettinari, F. Marchetti, F. Condello, C. Pettinari, G. Lupidi, R. Scopelliti, S. Mukhopadhyay, T. Riedel and P. J. Dyson, *ORGANOMETALLICS*, 2014, 33, 3709–3715, and references cited therein.
26. A. Valentini, F. Conforti, A. Crispini, A. De Martino, R. Condello, C. Stellitano, G. Rotilio, M. Ghedini, G. Federici, S. Bernardini and D. Pucci, *J. MED. CHEM.*, 2009, 52, 484–491.